Carbohydrate Polymers 117 (2015) 771–777

Contents lists available at ScienceDirect

Carbohydrate Polymers

journal homepage: www.elsevier.com/locate/carbpol

Green synthesis of biocompatible carboxylic curdlan-capped gold nanoparticles and its interaction with protein

Jing-Kun Yan[a,*], Jin-Lin Liu[a], Yu-Jia Sun[a], Shuang Tang[a], Zheng-Ying Mo[a], Yuan-Shuai Liu[b,*]

[a] School of Food & Biological Engineering, Jiangsu University, Zhenjiang 212013, China
[b] Department of Chemical and Biomolecular Engineering, The Hong Kong University of Science and Technology, Clear Water Bay, Kowloon, Hong Kong

ARTICLE INFO

Article history:
Received 13 August 2014
Received in revised form
27 September 2014
Accepted 16 October 2014
Available online 30 October 2014

Keywords:
Carboxylic curdlan
Gold nanoparticles
Green synthesis
Structure
Protein-nanoparticle interaction

ABSTRACT

This study demonstrates a facile, green strategy for the preparation of gold nanoparticles (AuNPs) from chloroauric acid ($HAuCl_4$) using carboxylic curdlan (Cc) as both reducing and stabilizing agent. The as-prepared AuNPs are characterized by UV–vis spectroscopy, high resolution transmission electron microscopy, X-ray diffraction, energy dispersive X-ray spectrometry and Fourier transform infrared spectroscopy. The results indicated that the particle size of the AuNPs changes with variations in the reaction time and concentrations of Cc and $HAuCl_4$. The spherical AuNPs are well dispersed, exhibiting high stability even after six months storage. The carboxylic groups (COO^-) in the Cc molecules tend to adsorb and stabilize the surface of the AuNPs. The interaction between BSA and the Cc-capped AuNPs was investigated using fluorescence and circular dichroism spectroscopies. The results indicated that the BSA molecules adsorb on the surface of the AuNPs, without significant change in its helical structure even after conjugation with the AuNPs.

1. Introduction

Metal nanoparticles, especially gold nanoparticles (AuNPs), have recently gained significant attentions because of their unique properties and potential applications in catalysis, optoelectronics, sensors, biotechnology, and biomedicine (Daniel & Astruc, 2004; Dykman & Khlebtsov, 2012; Li, Zhao, & Astruc, 2014; Sau, Rogach, Jackel, Klar, & Feldmann, 2010; Yeh, Creran, & Rotello, 2012). In order to explore the biological processes that are critical for diagnostics and modulation of cell functions, a lot of work has been done on unraveling the surface interaction of biomolecules with metal nanoparticles (NPs) (Lacerda et al., 2010). Obviously, AuNPs are the natural starting points for understanding the protein-NP interactions due to their promise for diverse biomedical applications, such as molecular diagnostics, bioengineering, biomolecular imaging, and drug delivery for cancer therapeutics (Andres et al., 1996; Galletto, Brevet, Girault, Antoine, & Broyer, 1999; Ghosh, Han, De, Kim, & Rotello, 2008; Mirkin, Letsinger, Mucic, & Storhoff, 1996; Burt, Gutierrez-Wing, Miki-Yoshida, & Jose-Yacaman, 2004).

To date, AuNPs are being synthesized with a variety of bottom-up methods and technologies, including chemical reduction (Chen, Wang, Ballato, Foulger, & Carroll, 2003), seed-growth (Busbee, Obare, & Murphy, 2003), photochemistry (Kim, Song, & Yang, 2002), electrochemistry (Ye, Yan, Ye, & Zhou, 2010), sonochemistry (Qiu, Zhu, & Chen, 2003), and template-assisted supramolecular chemistry (Lehn, 1995). Among these techniques, the chemical reduction method, which involves the use of various reducing agents, such as hydrazine, sodium borohydride ($NaBH_4$), dimethyl formamide (DMF), and other organic compounds, is considered as the most simple and conventional method for the preparation of AuNPs. However, these reducing agents are often associated with potential environmental toxicity or biological hazards. Therefore, more and more interests are being put on the development of "green" synthesis strategies for the preparation of AuNPs using non-toxic, environmentally friendly and renewable materials.

Polysaccharides derived from renewable sources, including plants, animals, and microorganisms, are being extensively studied in a wide variety of biomedical applications and functional foods due to their notable and excellent bioactivities, such as immunostimulatory, antitumor, and antioxidant activities (Giavasis, 2014; Stachowiak & Reguła, 2012). In particular, polysaccharides possessing good biocompatibility and biodegradability play an important role in nanoscience and drug delivery owing to the presence of a large number of functional groups, including hydroxyl, carboxyl,

* Corresponding authors at: Jiangsu University, School of Food and Biological Engineering, 301, Xuefu Road, Zhenjiang 212013, China.
Tel.: +08615952819661/+852 23588409.
E-mail addresses: jkyan_27@163.com (J.-K. Yan), keysliu@ust.hk (Y.-S. Liu).

http://dx.doi.org/10.1016/j.carbpol.2014.10.048
0144-8617/

and amino groups, in their structures. Raveendran, Fu, and Wallen (2003) first reported a facile "green" method for the synthesis of metal nanoparticles using glucose as the reducing agent and starch as the protecting agent. Then many other polysaccharides and their derivatives have been employed for the "green" synthesis of AuNPs, such as chitosan (Huang et al., 2007), dextran (Wang, Zhan, & Huang, 2010), pullulan (Choudhury, Malhotra, Bhattacharjee, & Prasad, 2014), glucan (Jia, Xu & Zhang, 2013; Sen, Maity, & Islam, 2013), cellulose (Tan et al., 2010), and guar gum (Pandey, Goswami, & Nanda, 2013). Our group has also successfully developed a facile, simple, and eco-friendly method to synthesize silver nanoparticles (AgNPs) using aqueous solution of carboxylic curdlan (Cc), which was prepared by the 4-acetamido-2,2,6,6-tetramethypiperidine-1-oxyl radical-mediated oxidation curdlan, as both reducing and stabilizing agents (Yan et al., 2013). However, no studies have been reported on the green synthesis of AuNPs using Cc solution. Herein, for the first time, we developed a green strategy for the synthesis of AuNPs from chloroauric acid ($HAuCl_4$) using Cc as the reducing as well as stabilizing agent. The characteristics and mechanism of the as-prepared Cc-AuNPs have been systematically elucidated using UV–vis spectroscopy, high-resolution transmission electron microscopy (HR-TEM), X-ray diffraction (XRD), energy-dispersive X-ray (EDX) analysis, and Fourier-transform infrared (FT-IR) spectroscopy. In addition, the interaction between the prepared Cc-AuNPs and bovine serum albumin (BSA) has been investigated using fluorescence spectroscopy and circular dichroism (CD) spectroscopy.

2. Materials and methods

2.1. Materials and chemicals

Carboxylic curdlan (Cc) bearing the β-1,3-polyglucuronic acid structure was prepared from 4-acetamido-TEMPO-mediated oxidation, details being shown in our previous work (Yan et al., 2014). The carboxylate content and molecular weight (M_W) of Cc are 4.87 mmol/g and 1.2×10^5 Da, respectively. Hydrogen tetrachloroaurate(III) tetrahydrate ($HAuCl_4 \cdot 3H_2O$, 99%), and bovine serum albumin (BSA, MW 6.6×10^4 kDa) were obtained from Sigma-Aldrich Chemical Co. (St. Louis, MO, USA). All other chemicals and solvents were of laboratory grade, without further purification. Ultrapure Milli-Q water (18.2 MΩ cm at 25 °C) was used in all experiments.

2.2. Green synthesis of Cc-capped gold nanoparticles (Cc-AuNPs)

Stock solutions of $HAuCl_4$ with concentrations ranging from 0.5 to 2.0 mM were prepared by adding gold(III) chloride hydrate in deionized water. For the synthesis of AuNPs, 2 mL of the $HAuCl_4$ stock solution was added to an equal volume of Cc (0.2%, w/v). The resulting mixture was maintained at 100 °C under continuous stirring in a water bath for different reaction time (15–120 min) to obtain AuNPs.

2.3. Characterization

The UV–vis absorption spectra of the as-prepared Cc-AuNPs solutions were obtained from a Perkin-Elmer Lambda 35 spectrophotometer in the wavelength range of 400–700 nm with the interval of 1.0 nm. The change in the color was directly recorded by a digital camera. The particle size and morphology of the Cc-AuNPs was observed using high resolution transmission electron microscopy (HRTEM, Tecnai 12, Philips, 120 kV). For TEM analysis, the sample was prepared by placing a drop of the Cc-AuNPs solution on a carbon coated copper grid (300 meshes), followed by drying at room temperature (20 °C) for 30 min. The elemental composition

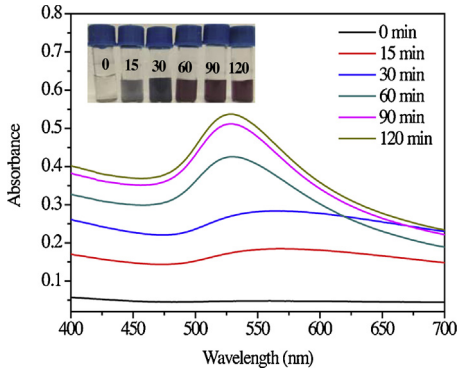

Fig. 1. UV–vis spectra absorption of Cc-AuNPs prepared with 0.2% (w/v) Cc and 2.0 mM $HAuCl_4$ at 100 °C for different reaction times (inset images: solution color in different time interval). (For interpretation of the references to color in this figure legend, the reader is referred to the web version of this article.)

of the nanoparticles was determined by an EDX spectroscope (Inca Energy-350, Oxford Co., UK) attached to the SEM (JSM-7001F, JEOL Ltd., Japan). The critical structure of the Cc-AuNPs was determined by a wide-angle XRD (D8-Advance, Bruker, Co., Germany). The XRD patterns were recorded with Cu $K\alpha$ radiation ($\lambda = 0.1541$ nm) at 40 kV and 40 mA in the 2θ ranging from 30° to 80° with a step speed of 4°/min. Fourier-transform infrared (FT-IR) spectra of Cc and freeze-dried Cc-AuNPs were obtained from a Nexus 670 FT-IR spectrometer (Thermo Nicolet Co., USA) in the wavenumber range of 500–4000 cm^{-1} with KBr pellets and referenced against air.

2.4. Preparation and characterization of Cc-AuNPs and BSA interactant

The interactant was prepared by adding 50 μL of the as-prepared Cc-AuNPs solution (with different concentrations ranging from 10^{-12} to 10^{-6} M) to 1 mL of BSA solution (0.01 mg/mL). Then the mixture was incubated at 25 °C in a water bath for 3 h under continuous stirring. After incubation, the mixture was maintained at 4 °C before analysis.

The fluorescence spectra of BSA and BSA/Cc-AuNPs interactants were recorded on a Perkin Elmer LS35 spectrofluorimeter in the wavelength range of 300–450 nm using the excitation wavelength of 290 nm. The width of both the excitation and emission slit was 5.0 nm. Furthermore, the CD spectra were recorded on a circular dichroism spectrometer (JASCO J-815, Japan) at room temperature using a 0.1 cm path length quartz cell in the wavelength range of 190–290 nm.

3. Results and discussion

3.1. Influence of reaction time on the synthesis of Cc-AuNPs

Owing to the presence of a large number of hydroxyl and carboxyl (COO^-) groups, the Cc molecules prepared via the 4-acetamido-TEMPO-mediated oxidation of curdlan exhibited a strong ability to adsorb metallic cations. The Cc molecules thus played the role of both reducing and stabilizing agents for the one-pot, green synthesis of AuNPs in an aqueous medium. Moreover, the functional groups in the Cc molecules cover and passivate the surface of the AuNPs, thereby preventing any further aggregation (Liu, Raveendran, Qin, & Ikushima, 2005).

Fig. 1 shows the UV–vis absorption spectra of the AuNPs prepared with 0.2% (w/v) Cc and 2.0 mM $HAuCl_4$ solution at 100 °C for different time intervals. After 15 min of incubation, the UV–vis spectra show a broad absorption band at around 530 nm. When the incubation time increases from 15 to 90 min, the bands become

stronger. The appearance of this typical surface plasmon resonance (SPR) band of AuNPs further indicates the formation of Cc-AuNPs (Mulvaney, 1996). The inset image of Fig. 1 shows that the $HAuCl_4$ aqueous solution is colorless in the beginning, and with the ongoing of reaction, the color becomes dark-blue and then wine red, without the formation of precipitates. This indicates that Au^{3+} in the solution is reduced to Au^0 by the Cc molecules (Zhou et al., 2009). In general, metal nanoparticles with various shapes and sizes show different colors in solutions, therefore the shape of the nanoparticles can be visually evaluated. For instance, metallic gold is yellow, spherical AuNPs are wine red or purple, while gold nanorods are blue or black in solution (Burda, Chen, Narayanan, & El-Sayed, 2005; Thakor, Jokerst, Zavaleta, Massoud, & Gambhir, 2011). These results also reveal that the Cc molecules in the solution could act as both reducing and stabilizing agents for the synthesis of well-dispersed spherical AuNPs, without the need of any additional reducing agents or stabilizers. In addition, no significant increase in absorption intensity could be observed after 90 min of reaction time, suggesting that the reaction is completed within 90 min.

3.2. Influence of Cc concentration on the synthesis of Cc-AuNPs

According to our previous work (Yan et al., 2013), the concentration of Cc has a significant influence on the formation of AgNPs. Therefore, in the present study, we analyzed the effects of Cc concentration on the synthesis of the as-prepared AuNPs. Fig. 2 shows the UV–vis absorption spectra of the AuNPs prepared with different concentrations of Cc (0.05% to 0.2%, w/v) and 2.0 mM $HAuCl_4$ at 100 °C for 90 min. When the Cc concentration is below 0.1%, Au^{3+} was not sufficiently reduced and stabilized for the preparation of AuNPs. It was found that there is a gradual increase in the absorption intensity, by increasing the Cc concentration up to 0.2% (w/v). Moreover, the width of absorption peak gradually becomes narrower with the increase in the concentration of Cc from 0.1% to 0.2%

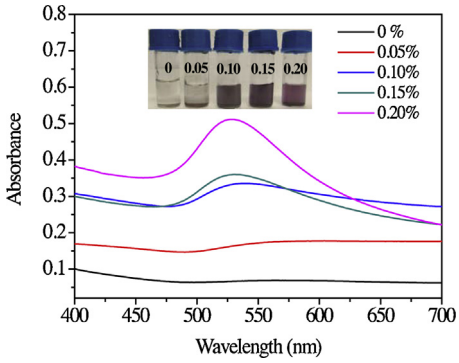

Fig. 2. UV–vis spectra absorption of Cc-AuNPs prepared with different concentrations of Cc and 2.0 mM $HAuCl_4$ at 100 °C for 90 min (inset images: solution color with different concentrations of Cc). (For interpretation of the references to color in this figure legend, the reader is referred to the web version of this article.)

(w/v) suggesting that the size distribution of the as-prepared AuNPs becomes narrower (Babapour, Akahavan, Azimirad, & Moshfeg, 2006). In addition, the SPR band of the as-synthesized AuNPs blue-shifted from 540 nm to 530 nm with increasing Cc concentration from 0.1% to 0.2% (w/v) indicating that the particle size was decreased with increasing Cc concentration. In addition, the effect of Cc concentration on the formation of AuNPs was also evaluated by visually observing the color changes in the solution. As can be seen from the inset image shown in Fig. 2, the color of the solution changes from colorless to light blue or blue color and subsequently to wine red color with increase in the concentration of Cc from 0.05% to 0.2%. This indicates that the shape of the as-prepared particles can be tuned by controlling the concentration of Cc. In the present study, the concentration of Cc suitable for the preparation of AuNPs was found to be 0.2% (w/v). Neither AuNP aggregation nor polymer phase separation was observed under this condition.

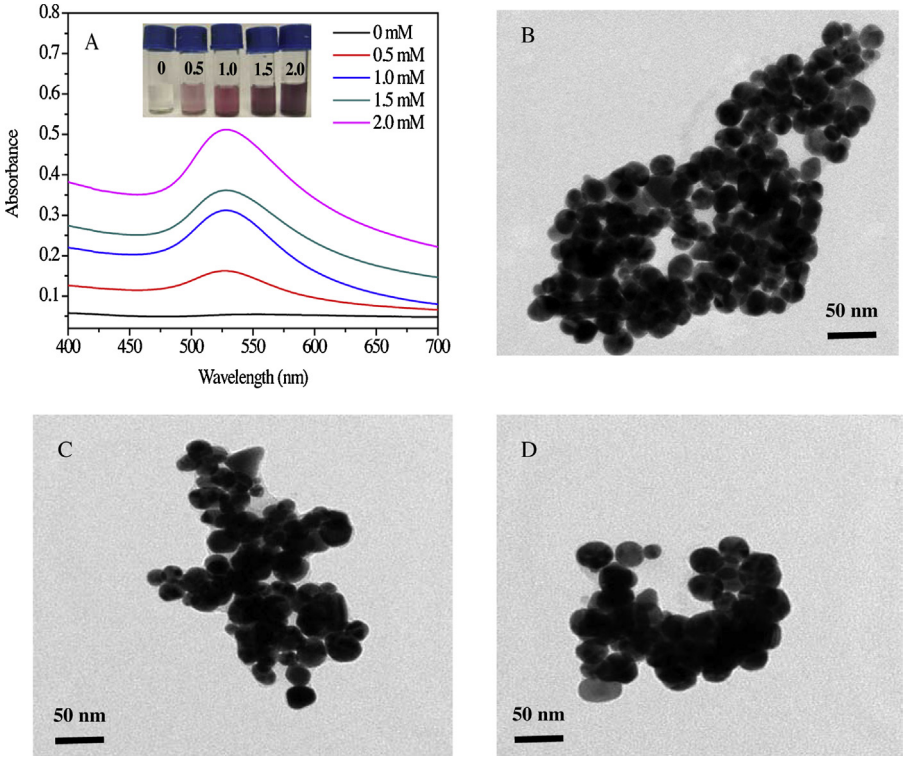

Fig. 3. (A) UV–vis spectra absorption of Cc-AuNPs prepared with 0.2% (w/v) Cc and different concentrations of $HAuCl_4$ at 100 °C for 90 min (inset images: solution color with different concentrations of $HAuCl_4$); HRTEM images of Cc-AuNPs prepared with 0.2% (w/v) Cc and 0.5 mM $HAuCl_4$ (B), 1.0 mM $HAuCl_4$ (C), and 2.0 mM $HAuCl_4$ (D). (For interpretation of the references to color in this figure legend, the reader is referred to the web version of this article.)

3.3. Influence of $HAuCl_4$ concentration on the synthesis and morphology of the Cc-AuNPs

Fig. 3A shows the UV–vis absorption spectra of the AuNPs prepared by reducing different concentrations of $HAuCl_4$ solution with 0.2% (w/v) Cc at 100 °C for 90 min. The absorption peaks appear at about 530 nm, which is a characteristic SPR band of AuNPs and confirms the formation of AuNPs under different concentrations of $HAuCl_4$ solution. With an increase in the concentration of $HAuCl_4$ from 0.5 to 2.0 mM, the intensity of the absorption peak increased gradually, suggesting the formation of more nanoparticles at higher concentration of $HAuCl_4$. Meanwhile, the effects of $HAuCl_4$ concentration on the formation of AuNPs can also be visually observed through the color change of the solution. As shown in the inset images of Fig. 3A, the AuNPs formed under lower concentration of $HAuCl_4$ (0.5 mM) exhibits a light purple color in solution, and the color becomes deeper to wine red or purple at higher concentration (2.0 mM).

The particle size and morphology of the AuNPs, formed by reducing 0.5, 1.0, and 2.0 mM $HAuCl_4$ solution with 0.2% (w/v) Cc, respectively, was recorded by HR-TEM (Fig. 3B–D). Fig. 3B shows the formation of well-dispersed spherical particles with an average size of ~17 nm, at the $HAuCl_4$ concentration of 0.5 mM. When $HAuCl_4$ concentration increases to 2.0 mM, the particle size also increased to 24 nm (Fig. 3D), correspondingly, higher concentration of $HAuCl_4$ leading to the formation of larger sized AuNPs. This result agrees well with the UV–vis analysis and visual observation of color formation. It is reasonable because higher concentration of Au^{3+} ions in the $HAuCl_4$ solution provides more nuclei, which favors further growth of the nanoparticles (Wu, Zhang, & Zhang, 2012). More specifically, an increase in the concentration of $HAuCl_4$ may result in the aggregation of particles to some extent, perhaps due to the role of polysaccharides as stabilizers or nucleating agents (Sen et al., 2013). The amount of 0.2% (w/v) Cc used in this work is sufficient enough to reduce the Au^{3+} ions in the high $HAuCl_4$ concentration of 2.0 mM, but could not completely prevent the aggregation of the as-formed AuNPs. However, at lower concentrations, the same concentration of Cc is completely sufficient to stabilize the AuNPs and prevent further aggregation, forming smaller size of AuNPs.

3.4. Characterization of Cc-AuNPs through XRD and EDX

Fig. 4A shows the XRD pattern of the AuNPs prepared with 0.2% (w/v) Cc and 2.0 mM $HAuCl_4$ solution at 100 °C for 90 min. The four diffraction peaks at 2θ corresponding to 38.2°, 44.4°, 64.6°, and 77.7° can be attributed to the (1 1 1), (2 0 0), (2 2 0), and (3 1 1) planes, respectively, of the face-centered cubic (fcc) gold. The Bragg reflections (2 0 0), (2 2 0), and (3 1 1) are relatively weaker and broader compared to the intense (1 1 1) reflection, implying that the gold nanocrystals are preferentially oriented along the (1 1 1) plane. The EDX spectrum of the AuNPs (Fig. 4B) reveals a strong and typical optical absorption peak at approximately 200 eV, which could be attributed to the SPR of the metallic Au nanocrystals, and confirms the formation of AuNPs in the reaction medium. In addition, the presence of Au, C, and O elements in the EDX spectrum indicates that the nanocomposite consists of both Cc and AuNPs.

3.5. FT-IR analysis and mechanism underlying the formation of Cc-AuNPs

Fig. 5 shows the FT-IR spectra of Cc and Cc-AuNPs prepared from 0.2% (w/v) Cc and 2.0 mM $HAuCl_4$ at 100 °C for 90 min, aiming to investigate the possible interaction between the Cc molecules and the Cc-capped AuNPs in the solution. The FT-IR spectrum of Cc (Fig. 5A) shows two characteristic absorptions of the polysaccharides. The strong and wide stretching peak at approximately

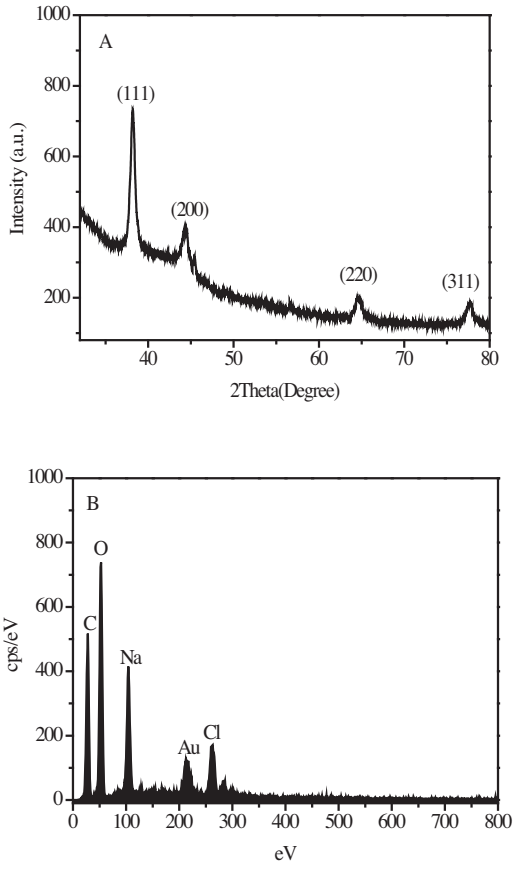

Fig. 4. (A) XRD pattern of Cc-AuNPs; (B) EDX of Cc-AuNPs. Cc-AuNPs prepared with 0.2% (w/v) Cc and 2 mM $HAuCl_4$ at 100 °C for 90 min.

3470 cm^{-1} can be ascribed to the O—H stretching vibration, while the weak absorption peak at approximately 2935 cm^{-1} can be associated with the C—H stretching vibration. The absorption band at 1636 cm^{-1} can be attributed to the asymmetrical COO^- stretching vibration, and that at 1426 cm^{-1} to the symmetrical COO^- stretching vibration (Delattre et al., 2009). The absorption peaks at 1087 and 1050 cm^{-1} are ascribed to the stretching vibration of C—OH. Additional peaks at 3450, 2932, 1632, 1426, 1087, and 1050 cm^{-1} (Fig. 5B) correspond to O—H, C—H, COO^- and C—OH, respectively, coincident with the characteristic peaks of the polysaccharides. This suggests that the skeleton structure of Cc remains unaltered after the formation of AuNPs. Interestingly, a new peak appeared at around 1730 cm^{-1} can be ascribed to the stretching vibration of free —COOH group, indicating the reduction of Au^{3+} to Au^0 by the polysaccharide in the solution (Shi & Sun, 1988). Sun et al. (2008) has reported a number of glycosidic linkages in the polysaccharide chain are broken into shorter segments in an acidic $HAuCl_4$ solution. Besides, some —CHO groups, present in the opened structure, may be oxidized to —COOH groups along with the reduction of Au^{3+} to Au^0 in the presence of Au^{3+}. Moreover, the peak at 1636 cm^{-1} (COO^- stretching vibration) is slightly shifted towards 1632 cm^{-1} in the FT-IR spectrum of Cc-AuNPs, meaning that the combination between Au nanoparticles and Cc molecules is through affinity or electrostatic interaction with carboxylate (COO^-) groups, and leads to no traces of blank AuNPs in the suspension. Therefore, the functional groups present in the Cc molecules play a dual role of both reducing agent and stabilizing agent in synthesizing as well as protecting the as-formed AuNPs.

Our previous work have reported that the Cc molecules bearing the β-1,3-polyglucuronic acid structure existed as a semi-flexible chain in the aqueous solution and had the potential for producing

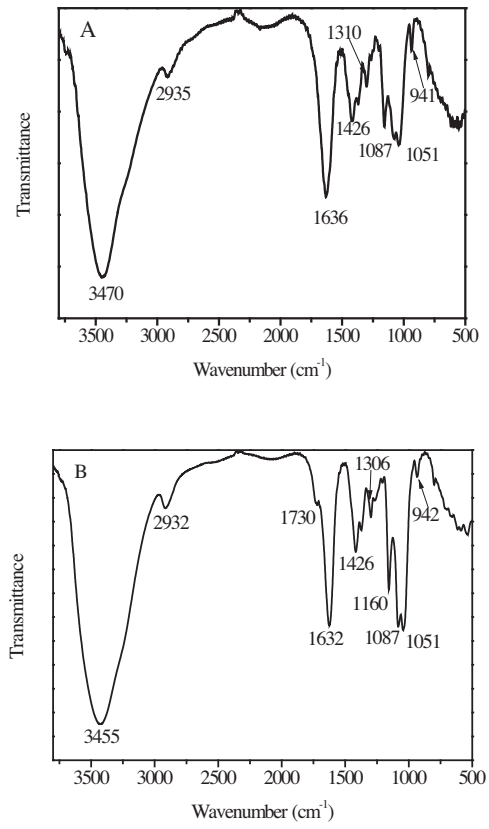

Fig. 5. FT-IR spectra of (A) Cc and (B) Cc-AuNPs synthesized in 0.2% (w/v) Cc and 2 mM $HAuCl_4$ at 100 °C for 90 min.

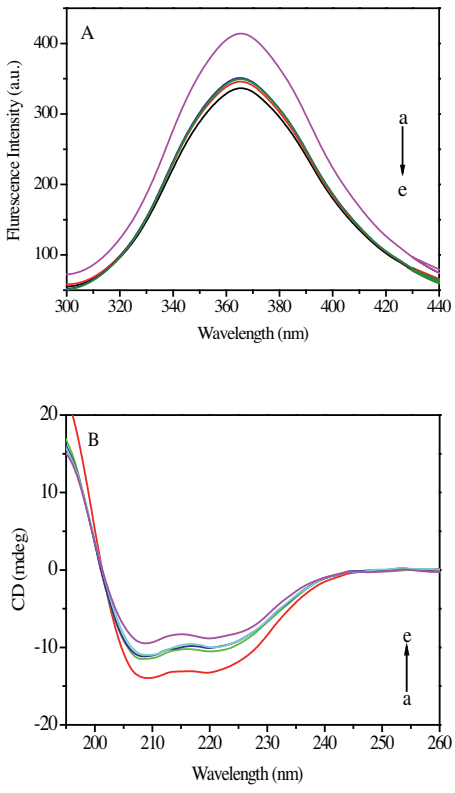

Fig. 7. (A) Fluorescence spectra of BSA in the presence of Cc-AuNPs. The concentrations of Cc-AuNPs are: (a) 0 M, (b) 10^{-12} M, (c) 10^{-10} M, (d) 10^{-8} M, and (e) 10^{-6} M; (B) CD spectra of native BSA (curve a) and BSA conjugated with different concentrations of Cc-AuPNs: (b). 10^{-12} M, (c) 10^{-10} M, (d) 10^{-8} M, and (e) 10^{-6} M.

gene carriers, bio-nanomaterials, and other chiral nanowires, through hydrogen bonding interactions, hydrophobic interactions, and electrostatic attraction (Yan et al., 2014; Lien et al., 2011). Based on this study, a possible mechanism underlying the green synthesis of AuNPs is proposed in Fig. 6, Cc serving both as a reducing agent as well as a capping agent for the synthesis and stabilization of AuNPs. First, the extensive carboxylic groups (COO^-) on the C-6 position of the Cc chains play an active role in the adsorption and stabilization of the Au^{3+} ions through electrostatic attraction or affinity interaction. Second, the hydroxyl groups in the Cc chain reduce the adsorbed Au^{3+} ions to Au^0 and metallic Au, which further nucleate and grow to form AuNPs. The AuNPs are subsequently capped and stabilized by Cc because of its oxygen-rich structure (Huang et al., 2007). Meanwhile, the hydroxyl groups in the polymeric chains and networks will also promote the stabilization of the AuNPs. The AuNPs formed by this method are highly stable and well dispersed, and there is no any color change or precipitates formation after six months of storage at room temperature from direct visual observation.

3.6. Studies on the interaction of Cc with BSA

Generally, the adsorption of proteins on the surface of the NPs alters the surface functionality and thus may strongly influence the translocation behavior in the biological systems (Treuel, Malissek, Gebauer, & Zellner, 2010). In order to understand the fate of the NPs in the biological systems, we analyzed the interactions between BSA and the AuNPs prepared from 0.2% (w/v) Cc and 2 mM $HAuCl_4$ at 100 °C for 90 min using fluorescence spectroscopy and CD measurements. Fig. 7A show that the fluorescence intensity of BSA at around 365 nm (the presence of tyrosine, tryptophan, and phenylalanine residues in BSA molecule), tends to decrease when the concentration of Cc-AuNPs increases from 10^{-12} M to

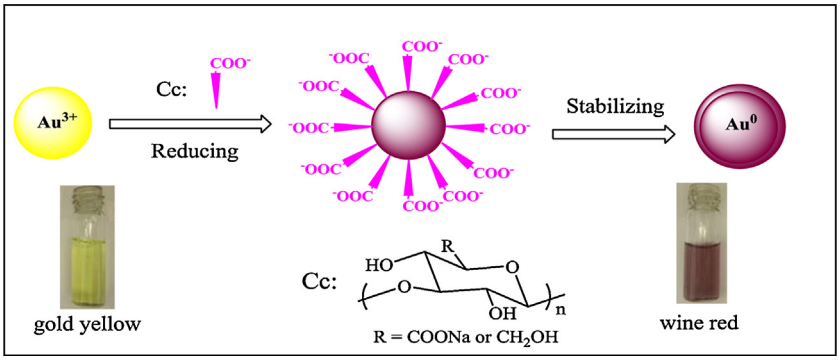

Fig. 6. Proposed scheme for the preparation of AuNPs by Cc.

10^{-6} M, suggesting that the addition of Cc-AuNPs quenches BSA fluorescence emission, without any peak shift or the formation of new peak. The observed quenching of the fluorescence intensity of BSA may be attributed to the formation of conjugate between Cc-AuNPs and BSA.

CD is powerful in studying the interactions of proteins with other molecules and investigating the protein conformation in solution or adsorbed onto other molecules. In general, the presence of high percentage of α-helical (67%) structure in the BSA molecules exhibits a characteristic CD signal in the far UV region. Typically, changes in the ellipticity at 208 and 222 nm are considered useful probes for visualizing the variations in α-helical content. Fig. 7B shows the CD spectra of BSA in the absence and presence of different concentrations of AuNPs. The ellipticity at 208 and 222 nm of BSA gradually decrease with an increase in the concentration of Cc-AuNPs from 10^{-12} M to 10^{-6} M, implying that the AuNPs capped with the carboxylic groups of Cc influence the conformation of BSA to a certain extent. Nonetheless, the change in α-helical content of BSA is not significant even after conjugation with 10^{-6} M AuNPs. It is well known that the changes in the original structure of the protein result in loss of biological activity or the activation of immune response (Brandes, Welzel, Werner, & Kroh, 2006). Remarkably, the BSA molecule could maintain most of its α-helical structure after conjugation in this study, which offers great potentials as a novel carrier of proteins for biomedical applications.

4. Conclusions

In summary, we developed a facile and green method for the preparation of well-dispersed spherical AuNPs using Cc as both reducing agent and stabilizing agent in aqueous medium. The particle size, shape, morphology, structure and elemental composition of the as-prepared AuNPs were thoroughly characterized using UV–vis spectroscopy, HRTEM, XRD, and EDX analyses, and the interactions between Cc and AuNPs were examined using FT-IR spectroscopy. Based on the FT-IR analysis, we proposed the possible mechanism underlying the synthesis of Au nanoparticles using Cc. In addition, the interaction between BSA and the Cc-capped AuNPs was also investigated using fluorescence spectroscopy and CD spectroscopy. The results suggest the potential use of non-toxic, benign, biodegradable, and biocompatible Cc as a reducing agent as well as stabilizer for the synthesis of metal nanoparticles, and a broad spectrum of their potential applications in biomedicine and bioanalytical fields.

Acknowledgements

This work was supported financially by the Natural Science Foundation of Jiangsu Province (BK20140542), China Postdoctoral Science Foundation funded project (2013M531292), the Priority Academic Program Development (PAPD) of Jiangsu Higher Education Institutions, and Jiangsu university students' scientific research project (13A097).

References

Andres, R. P., Bein, T., Dorogi, S., Feng, S., Henderson, J. I., Kubiak, C. P., et al. (1996). Coulomb staircase at room temperature in a self-assembled molecular nanostructure. *Science*, *272*, 1323–1325.

Babapour, A., Akahavan, O., Azimirad, R., & Moshfeg, A. Z. (2006). Physical characteristics of heat-treated nano-silvers dispersed in sol–gel silica matrix. *Nanotechnology*, *17*, 763–771.

Brandes, N., Welzel, P. B., Werner, C., & Kroh, L. W. (2006). Adsorption-induced conformational changes of proteins onto ceramic particles: Differential scanning calorimetry and FTIR analisys. *Journal of Colloid and Interface Science*, *299*, 56–69.

Burda, C., Chen, X., Narayanan, R., & El-Sayed, M. A. (2005). Chemistry and properties of nanocrystals of different shapes. *Chemical Reviews*, *105*, 1025–1102.

Burt, J. L., Gutierrez-Wing, C., Miki-Yoshida, M., & Jose-Yacaman, M. (2004). Noble-metal nanoparticles directly conjugated to globular proteins. *Langmuir*, *20*, 11778–11783.

Busbee, B. D., Obare, S. O., & Murphy, C. J. (2003). An improved synthesis of high-aspect-ratio gold nanorods. *Advanced Materials*, *15*(5), 414–416.

Chen, S., Wang, Z. L., Ballato, J., Foulger, S. H., & Carroll, D. L. (2003). Monopod, bipod, tripod, and tetrapod gold nanocrystals. *Journal of the American Chemical Society*, *125*(52), 16186–16187.

Choudhury, A. R., Malhotra, A., Bhattacharjee, P., & Prasad, G. S. (2014). Facile and rapid thermo-regulated biomineralization of gold by pullulan and study of its thermodynamic parameters. *Carbohydrate Polymers*, *106*, 154–159.

Daniel, M. C., & Astruc, D. (2004). Quantum-size-related properties, and applications toward biology, catalysis and nanotechnology. *Chemical Reviews*, *104*, 293–346.

Delattre, C., Rios, L., Laroche, C., Le, N. H. T., Lecerf, D., Picton, L., et al. (2009). Production and characterization of new families of polyglucuronic acids from TEMPO–NaOCl oxidation of curdlan. *International Journal of Biological Macromolecules*, *45*, 458–462.

Dykman, L., & Khlebtsov, N. (2012). Gold nanoparticles in biomedicinal applications: Recent advances and perspectives. *Chemical Society Reviews*, *41*, 2256–2282.

Galletto, P., Brevet, P. F., Girault, H. H., Antonine, R., & Broyer, M. (1999). Enhancement of the second harmonic response by adsorbates on gold colloids: The effect of aggregation. *Journal of Physical Chemistry B*, *103*, 8706–8710.

Ghosh, P., Han, G., De, M., Kim, C. K., & Rotello, V. M. (2008). Gold nanoparticles in delivery applications. *Advanced Drug Delivery Reviews*, *60*, 1307–1315.

Giavasis, I. (2014). Bioactive fungal polysaccharides as potential functional ingredients in food and nutraceuticals. *Current Opinion in Biotechnology*, *26*, 162–173.

Huang, L., Zhai, M., Peng, J., Xu, L., Li, J., & Wei, G. (2007). Synthesis, size control and fluorescence studies of gold nanoparticles in carboxymethylated chitosan aqueous solutions. *Journal of Colloid and Interface Science*, *316*, 398–404.

Jia, X., Xu, X., & Zhang, L. (2013). Synthesis and stabilization of gold nanoparticles induced by denaturation and renaturation of triple helical β-glucan in water. *Biomacromolecules*, *14*, 1787–1794.

Kim, F., Song, J. H., & Yang, P. (2002). Photochemical synthesis of gold nanorods. *Journal of the American Chemical Society*, *124*(48), 14316–14317.

Lacerda, S. H. D. P., Park, J. J., Meuse, C., Pristinski, D., Becker, M. L., Karim, A., et al. (2010). Interaction of gold nanoparticles with common human blood proteins. *ACS Nano*, *4*, 365–379.

Lehn, J. M. (1995). *Supramolecular Chemistry. Concepts and Perspectives*. Weinheim: VCH.

Li, N., Zhao, P., & Astruc, D. (2014). Anisotropic gold nanoparticles: Synthesis, properties, applications, and toxicity. *Angewandte Chemie International Edition*, *53*, 2–36.

Lien, L. T. N., Shiraki, T., Dawn, A., Tsuchiya, Y., Tokunaga, D., Tamaru, S., Enomoto, N., Hojo, J., & Shinkai, S. (2011). A pH-responsive carboxylic β-1,3-glucan polysaccharide for complexation with polymeric guests. *Organic & Biomolecular Chemistry*, *9*, 4266–4275.

Liu, J., Raveendran, P., Qin, G., & Ikushima, Y. (2005). Self-asembly of beta-D glucose-stabilized Pt nanocrystals into nanowire-like structures. *Chemical Communications*, *23*, 2972–2974.

Mirkin, C. A., Letsinger, R. L., Mucic, R. C., & Storhoff, J. J. (1996). A DNA-based method for rationally assembling nanoparticles into macroscopic materials. *Nature*, *382*, 607–609.

Mulvaney, P. (1996). Surface plasmon spectroscopy of nanosized metal particles. *Langmuir*, *12*, 788–800.

Pandey, S., Goswami, G. K., & Nanda, K. K. (2013). Green synthesis of polysaccharide/gold nanoparticles nanocomposite: An efficient ammonia sensor. *Carbohydrate Polymers*, *94*, 229–234.

Qiu, X. F., Zhu, J. J., & Chen, H. Y. (2003). Controllable synthesis of nanocrystalline gold assembled whiskery structures via sonochemical route. *Journal of Crystal Growth*, *257*, 378–383.

Raveendran, P., Fu, J., & Wallen, S. L. (2003). Completely green synthesis and stabilization of mental nanoparticles. *Journal of the American Chemical Society*, *125*, 13940–13941.

Sau, T. K., Rogach, A. L., Jackel, F., Klar, T. A., & Feldmann, J. (2010). Properties and applications of colloidal nonspherical nobel metal nanoparticles. *Advanced Materials*, *22*, 1805–1825.

Sen, I. K., Maity, K., & Islam, S. S. (2013). Green synthesis of gold nanoparticles using a glucan of an edible mushroom and study of catalytic activity. *Carbohydrate Polymers*, *91*, 518–528.

Shi, Y., & Sun, X. (1988). *Spectrum and chemical identification of organic compounds*. Nanjing: Jiangsu Science Technology Press.

Stachowiak, B., & Reguła, J. (2012). Health-promoting potential of edible macromycetes under special consideration of polysaccharides: A review. *European Food Research and Technology*, *234*, 369–380.

Sun, C., Qu, R., Chen, H., Ji, C., Wang, C., Sun, Y., et al. (2008). Degradation behavior of chitosan chains in the green synthesis of gold nanoparticles. *Carbohydrate Research*, *343*, 2595–2599.

Tan, J., Liu, R., Wang, W., Liu, W., Tian, Y., Wu, M., et al. (2010). Controllable aggregation and reversible pH sensitivity of AuNPs regulated by carboxymethyl cellulose. *Langmuir*, *26*(3), 2093–2098.

Thakor, A., Jokerst, J., Zavaleta, C., Massoud, T., & Gambhir, S. (2011). Gold nanoparticles: A revival in precious metal administration to patients. *Nano Letters*, *11*, 4029–4036.

Treuel, L., Malissek, M., Gebauer, J. S., & Zellner, R. (2010). The influence of surface composition of nanoparticles on their interactions with serum albumin. *ChemPhysChem*, *11*, 3093–3099.

Wang, Y., Zhan, L., & Huang, C. Z. (2010). One-pot preparation of dextran-capped gold nanoparticles at room temperature and colorimetric detection of dihydralazine sulfate in uric samples. *Analytical Methods*, *2*, 1982–1988.

Wu, J., Zhang, F., & Zhang, H. (2012). Facile synthesis of carboxymethyl curdlan-capped silver nanoparticles and their applications in SERS. *Carbohydrate Polymers*, *90*, 261–269.

Yan, J. K., Cai, P. F., Cao, X. Q., Ma, H. L., Zhang, Q., Hu, N. Z., et al. (2013). Green synthesis of silver nanoparticles using 4-acetamido-TEMPO-oxidized curdlan. *Carbohydrate Polymers*, *97*, 391–397.

Yan, J. K., Ma, H. L., Cai, P. F., Zhang, Q., Hu, N. Z., Feng, X. B., et al. (2014). Structural characteristics and antioxidant activities of different families of 4-acetamido-TEMPO-oxidized curdlan. *Food Chemistry*, *143*, 530–535.

Ye, W., Yan, J., Ye, Q., & Zhou, F. (2010). Template-free and direct electrochemical deposition of hierarchical dentritic gold microstructures: Growth and their multiple applications. *Journal of Physical Chemistry C*, *114*(37), 15617–15624.

Yeh, Y. C., Creran, B., & Rotello, V. M. (2012). Gold nanoparticles: Preparation, properties, and applications in bionanotechnology. *Nanoscale*, *4*, 1871–1880.

Zhou, M., Wang, B., Rozynek, Z., Xie, Z., Fossum, J. O., Yu, X., et al. (2009). Minute synthesis of extremely stable gold nanoparticles. *Nanotechnology*, *20*, 505606.